

# An experimental investigation of convection in a fluid that exhibits phase change

By D. E. FITZJARRALD†

Department of Land, Air and Water Resources, University of California, Davis, CA 95616

(Received 19 December 1979)

Convection flows have been systematically observed in a layer of fluid between two isothermal horizontal boundaries. The working fluid was a nematic liquid crystal, which exhibits a liquid–liquid phase change at which latent heat is released and the density changed. In addition to ordinary Rayleigh–Bénard convection when either phase is present alone, there exist two distinct types of convective motions initiated by the unstable density difference. When a thin layer of heavy fluid is present near the top boundary, hexagons with downgoing centres exist with no imposed thermal gradient. When a thin layer of light fluid is brought on near the lower boundary, the hexagons have upshooting centres. In both cases, the motions are kept going once they are initiated by the instability due to release of latent heat. Relation of the results to applicable theories is discussed.

## 1. Introduction

This paper reports the results of a laboratory experiment in convection flow through a phase change, across which the density changes and latent heat is released. The working fluid is a nematic liquid crystal that undergoes a first-order phase change at convenient temperature and pressure. The addition of a first-order phase change to the convection flow makes the problem much more interesting, because in addition to the thermal buoyancy  $g\beta\Delta T$  there are two more sources of buoyant acceleration, i.e. the latent heat release and density difference across the phase boundary. Thus, in addition to the ordinary Rayleigh number  $R_T = \Delta T\beta g d^3/\nu\kappa$ , there are two more very similar parameters. When the imposed temperature difference,  $\Delta T$ , is replaced by the temperature that is characteristic of the latent heat release,  $L/c_p$ , the governing parameter is  $R_L = (L/c_p)\beta g d^3/\nu\kappa$ . And when the density difference across the phase boundary,  $\Delta\rho$ , is used the parameter is  $R_{\Delta\rho} = (\Delta\rho/\rho)gd^3/\nu\kappa$ . In the above,  $\beta$  is the expansion coefficient,  $g$  is gravity,  $d$  is the layer depth,  $\nu$  and  $\kappa$  are the diffusivities of momentum and heat,  $L$  is the latent heat, and  $c_p$  is the specific heat at constant pressure.

The phase-change convection problem is further complicated by the fact that there are two possible geometries, even in the thermally unstable case (lower boundary hotter). When the lighter phase is present near the lower boundary, increases of both  $R_L$  and  $R_{\Delta\rho}$  are destabilizing, i.e. an increase in either parameter is similar to an increase in  $R_T$  and brings the flow closer to the point of marginal stability. The latent heat effect is due to the release of latent heat in the hot updraft regions, and the density

† Current affiliation: Geophysical Fluid Dynamics Institute, Florida State University, Tallahassee, Florida 32306.

effect occurs because the basic state is statically unstable, i.e., the Rayleigh–Taylor geometry. When the heavier fluid lies near the hotter lower boundary, increasing  $R_L$  is now stabilizing, since in the updrafts latent heat is taken in. Increasing  $R_{\Delta\rho}$  is destabilizing, since the phase boundary moves opposite to the vertical motion so that gravity, tending to flatten out the phase boundary, induces upward motion in the region of updraft. The latter effect was first shown by Busse & Schubert (1971), who demonstrated that the phase boundary in this case was not the barrier to motion that had been previously supposed (Knopoff 1964). In the above descriptions, it is assumed that the latent heat is released when the fluid goes from the lighter (higher temperature or lower pressure) phase to the heavier one, so that the heavier-above case applies to laboratory experiments where compressibility effects are negligible and the heavier-below case to the geophysical flows where such effects dominate.

Convection flows in which a fluid is thermally driven (Rayleigh–Bénard) and undergoes a phase change, or in which two immiscible fluids are driven by a density discontinuity (Rayleigh–Taylor) have a number of interesting applications to geophysics, meteorology, and astrophysics. Thermal convection through a phase boundary has been used to look at the problem of mantle convection that occurs in the presence of an olivine-spinel phase change at 400 km (Schubert & Turcotte 1971). The unstable two-fluid system has been used to explain the formation of geological structures such as salt domes (Whitehead & Luther 1974). In meteorology the latent heat release due to phase change is a crucial part in the description of cumulus convection and in cellular convection over the ocean, especially the closed-cell hexagonal convection occurring in marine stratocumulus layers (Schubert *et al.* 1979). In astrophysical flows the phase change process can be used to model convective flows in which heat is released from nuclear reactions or fluid properties changed due to ionization (Spiegel 1972).

The experiments reported here are necessarily limited to the heavier-above case, so the lighter phase must be present at the hotter lower boundary. Therefore, the conditions that can be examined are: thermal convection in each phase separately, convection with negligible thermal gradient and unstable phase boundary, and thermal convection including phase change. The goal of the work is to analyse the unique laboratory fluid flows obtained in the presence of a phase change. We will also see if the results, or other experiments using these fluids, can be used to understand geophysical flows with phase change.

We begin with thermal convection in each phase, also giving a brief review of the fluid dynamics of nematics, and then proceed to consider in turn each of the other cases possible in the laboratory.

## 2. Thermal convection in a single phase

The working fluid in the experiments described below exhibits a first-order phase change, i.e. one in which the density changes and latent heat is released. Above the phase-change temperature,  $T_c$ , the material is an ordinary isotropic fluid. Below  $T_c$  it is a nematic liquid crystal. Since we are interested primarily in the phase change, the experimental configuration and operating conditions will be chosen to minimize the effect of the unique anisotropies of the nematic phase. The single-phase experiments are presented both to provide a baseline with which to compare the two-phase results and to illustrate that the nematic anisotropies do not greatly affect the observed flows.

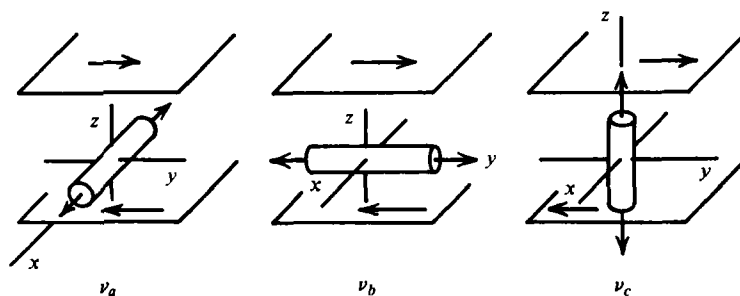


FIGURE 1. Sketch of the three principal viscosities,  $\nu_a$ ,  $\nu_b$ ,  $\nu_c$ , in a nematic.

## 2.2. Nematodynamics

A nematic liquid crystal is an anisotropic liquid made of long, rod-like molecules that can be aligned along one direction, designated by a unit vector  $\mathbf{n}$ . No change in properties is observed when  $\mathbf{n} \rightarrow -\mathbf{n}$ . When aligned, the direction of molecular orientation is easily determined, since the material is birefringent. The thermal and electrical conductivity, index of refraction, and viscosity all depend on the orientation of  $\mathbf{n}$  relative to the direction of propagation. Unlike isotropic fluids, nematics can resist torques elastically. The amount of elastic torque present in the fluid depends on the curvature of  $\mathbf{n}$ . The molecules can be aligned by imposing an electrical or magnetic field, by chemical alignment at the confining boundaries that is coupled to the interior by elastic torques, or by shears in the fluid. It is the last method of orientation that will be of interest in the present case.

The stress tensor of nematic fluids contains four viscosity coefficients in addition to that of ordinary isotropic fluids. It is also a function of  $\mathbf{n}$  (see deGennes 1974). The method of solution is to solve the ordinary Navier–Stokes equations for viscous flow, using the more complicated nematic stress tensor, together with an additional differential equation for  $\mathbf{n}$  that is the result of adding the torques on the molecules due to imposed fields, elastic torques, and fluid shears. When there are only small deviations in  $\mathbf{n}$  the analysis is considerably simplified, and a number of different flows have been solved. Shear instabilities (Dubois-Violette & Manneville 1978) and thermal convection (Guyon & Pieranski 1974, Guyon *et al.* 1979) in horizontal layers both give results that are unique to nematics. Thermal convection in a thin vertical slot when  $\mathbf{n}$  is normal to the confining boundaries has been solved by Horn *et al.* (1976) for the case when the orientation is due to elastic torques and by Fitzjarrald & Owen (1979) when an electrical field is imposed by a feedback circuit. The key to these successful solutions has been that the fluid exists in a thin layer or in the presence of an imposed field, so that there are only small deviations from a constant  $\mathbf{n}$ .

The present experiments are in thick layers with no imposed field, so in the interior of the fluid the dominant orienting mechanism is the fluid shear. The relative importance of shear and elastic torques has been discussed by Guyon *et al.* (1979). For example, in an electro-optic device with  $d \sim 10\mu\text{m}$  a fluctuation of orientation would take 0.1 s to be damped out by the elastic torques. When  $d \sim 1\text{ mm}$  (Fitzjarrald & Owen 1979) the corresponding time is 20 min, and in these experiments with  $d = 6.3\text{ mm}$  it would be 10 h. With a similar size cell ( $d = 5\text{ mm}$ ) Guyon *et al.* have used a strong magnetic field to maintain uniform orientation. Without this imposed field the viscous

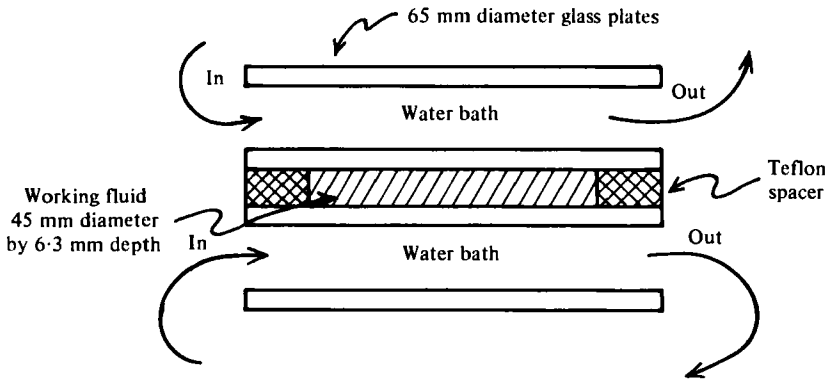


FIGURE 2. Sketch of convection cell.

torques align the molecules so that  $\mathbf{n}$  is parallel to the direction of motion (see de Gennes 1974). This makes shears visible because of birefringence and determines the effective viscosity of the fluid.

In simple shear flow there are three principal viscosities in a nematic, depending on the angle between  $\mathbf{n}$  and the shear. These are illustrated in figure 1. Near the phase-change temperature in a typical room-temperature nematic  $\nu_a$  is approximately the same as  $\nu_i$ , the isotropic value, while  $\nu_b$  is about 25% less than this value, and  $\nu_c$  is nearly double. So at the onset of motion in a randomly oriented nematic,  $\nu$  is slightly higher than in an isotropic fluid, since it is the average of the values for the three different orientations. As the motion starts, fluid shears are effective in orienting  $\mathbf{n}$ , so that the value of viscosity becomes very close to  $\nu_b$ . Therefore, there must be a slight decrease in viscosity as the motions start.

The thermal diffusivity is also anisotropic in a nematic, with the value of  $\kappa_{\parallel}/\kappa_{\perp} \sim 1.5$  for room-temperature nematics. Here  $\kappa_{\parallel}$  and  $\kappa_{\perp}$  are the diffusivities along and normal to  $\mathbf{n}$ , respectively. It is clear that, because of the two anisotropic effects—lowering of the effective viscosity and heat focusing by the anisotropic thermal diffusivity—the onset of motion in a convective cell will be considerably different in an initially well-ordered nematic than it is in an ordinary isotropic fluid. When shears are the dominant orienting mechanism, however, the flow should be similar to that of the isotropic phase, once the motion has started. In this case the viscosity becomes very nearly  $\nu_b$ , and since the convective heat transfer is greater than the conductive part, the conduction anisotropy is not a dominant effect.

In the experiments to follow, the peculiarities of nematics will be avoided by concentrating on the finite-amplitude flows that exist once the flow is well established. It may be noted that the result for a shear-oriented nematic is considerably different than for a uniformly-oriented one. When the molecules are initially oriented by an external field or surface treatment so that  $\mathbf{n}$  is parallel to the confining plates, the motion starts at  $R_t \sim 1$  instead of  $R_t \sim 1700$  for an isotropic fluid, because of the heat-focusing effect of the conductivity anisotropy (Guyon & Pieranski 1974). Coupling of the heat focusing to the thermal convection by means of changes in  $\mathbf{n}$  can also lead to oscillatory, or overstable convection because of the difference between the convection and orientation time scales (Guyon *et al.* 1979). And when  $\mathbf{n}$  is initially normal to the

plates, convective motions can occur when the fluid is heated from above (Guyon & Pieranski 1974).

### 2.2. Description of experiment

A sketch of the apparatus is shown in figure 2. The fluid is confined by means of glass plates in a horizontal layer 45 mm in diameter by 6.4 mm deep. Water is circulated to keep the confining plates at constant temperature. The conductivity of the glass is approximately 6 times that of the working fluid, and the water flow rates are large enough so that a nearly isothermal boundary condition is maintained. The working fluid is a cyanobiphenyl, *K-15* from BDH Chemicals. It is nematic from 22.5 to 35 °C, isotropic above 35 °C, and is very stable, being resistant to degradation by moisture, exposure to the atmosphere, and ultra-violet radiation. Unfortunately, not all the physical constants are known. The values that are known are very close to those of other room-temperature nematics (such as MBBA, more widely studied but much less stable), so that estimates of the unknown constants based on such typical values should be applicable to *K-15*. The physical properties of interest that are known for *K-15* are

$$\begin{aligned}\rho &= 1.02 \text{ g/cm}^3 \text{ at } 25^\circ \text{C}, \\ \beta &= 10^{-3} \text{ }^\circ\text{C}^{-1} \text{ at } 25^\circ \text{C}, \\ n_e/n_o &= 1.7/1.5 \text{ at } 25^\circ \text{C}, \\ L &\simeq 0.8 \text{ cal/g},\end{aligned}$$

where  $n_e$  and  $n_o$  are the extraordinary and ordinary indices of refraction, i.e. normal and parallel to  $\mathbf{n}$ . Properties of MBBA that should be approximately the same as *K-15* are:

$$\nu_i \sim 0.3 \text{ cm}^2 \text{ s}^{-1}, \quad \kappa_i \sim 10^{-3} \text{ cm}^2 \text{ s}^{-1}, \quad \Delta\rho/\rho \sim 2 \times 10^{-3}, \quad c_p \sim 0.4 \text{ cal g}^{-1} \text{ }^\circ\text{C}^{-1}.$$

We see that  $\Delta\rho/\rho$  and  $L/c_p$  both are approximately equal to a 2 °C change in fluid temperature. Using the above values, we find that  $\Delta T = 2^\circ \text{C}$  is enough to make  $R_T \approx 1700$  and initiate thermal convection. We find that motion starts with  $\Delta T \approx 1.5^\circ \text{C}$  in the isotropic phase just above  $T_c$ , so that the above values must be close to the true values. We intend to avoid the region near critical  $R_T$ , so that a more precise value of the constants is not necessary.

### 2.3. Thermal convection in one phase alone

With only one phase present and an unstable temperature gradient imposed, the familiar Rayleigh–Bénard results are obtained. Convection rolls are observed in both the nematic and isotropic phases when  $\Delta T$  exceeds some critical value, and the rolls are circular because of the circular symmetry of the experiment with downflow near the outer edge. In both cases upflow occurs at the centre of the experiment with 3 waves across the diameter, corresponding to a wavelength  $\lambda = 2.3d$ . However, the limited aspect ratio and the necessity of having an integer number of waves in the experiment precludes making any general conclusions from this measurement of the wavelength. Flow visualization in the clear isotropic (lighter) phase is by shadowgraph and interferometer that show the temperature distribution in the layer. In the liquid crystal (heavier) phase, the birefringence allows observation of the fluid motions. As soon as motion starts, the molecules line up along the direction of motion due to the action of

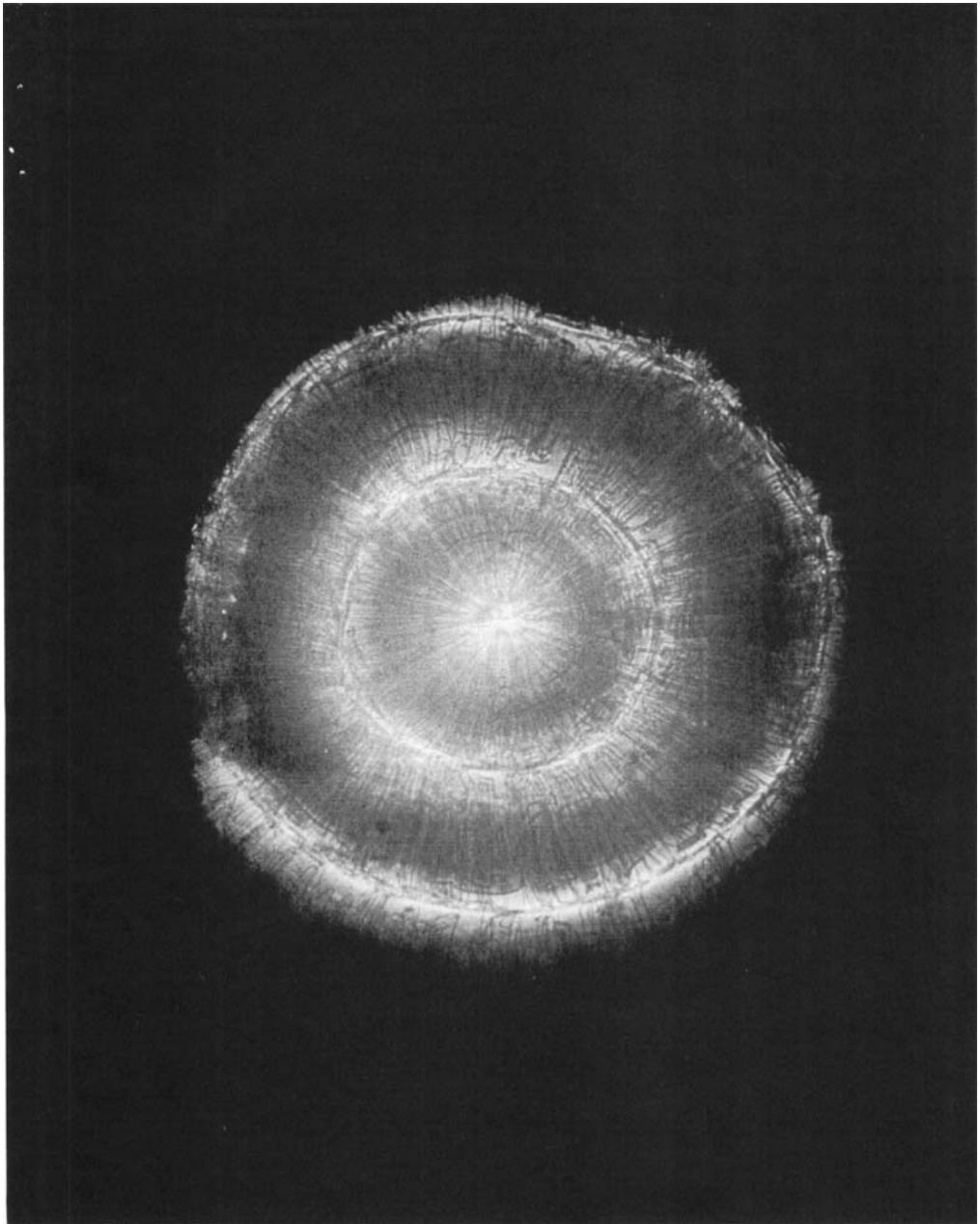


FIGURE 3. Thermal convection in liquid crystal phase alone.  $\Delta T = 2^\circ\text{C}$ . Transmitted monochromatic light is shown. Brighter areas are due to birefringence of the liquid crystal. Molecules are oriented by the fluid shears.

shear torques on  $\mathbf{n}$ . Thus, the fluid appears clear in the regions where it is moving directly toward or away from the observer, i.e. the hottest and coldest part of the convection rolls. In the region where the fluid is moving normal to the direction of viewing, the fluid appears opaque.

A photograph of monochromatic light transmitted through the convection cell is

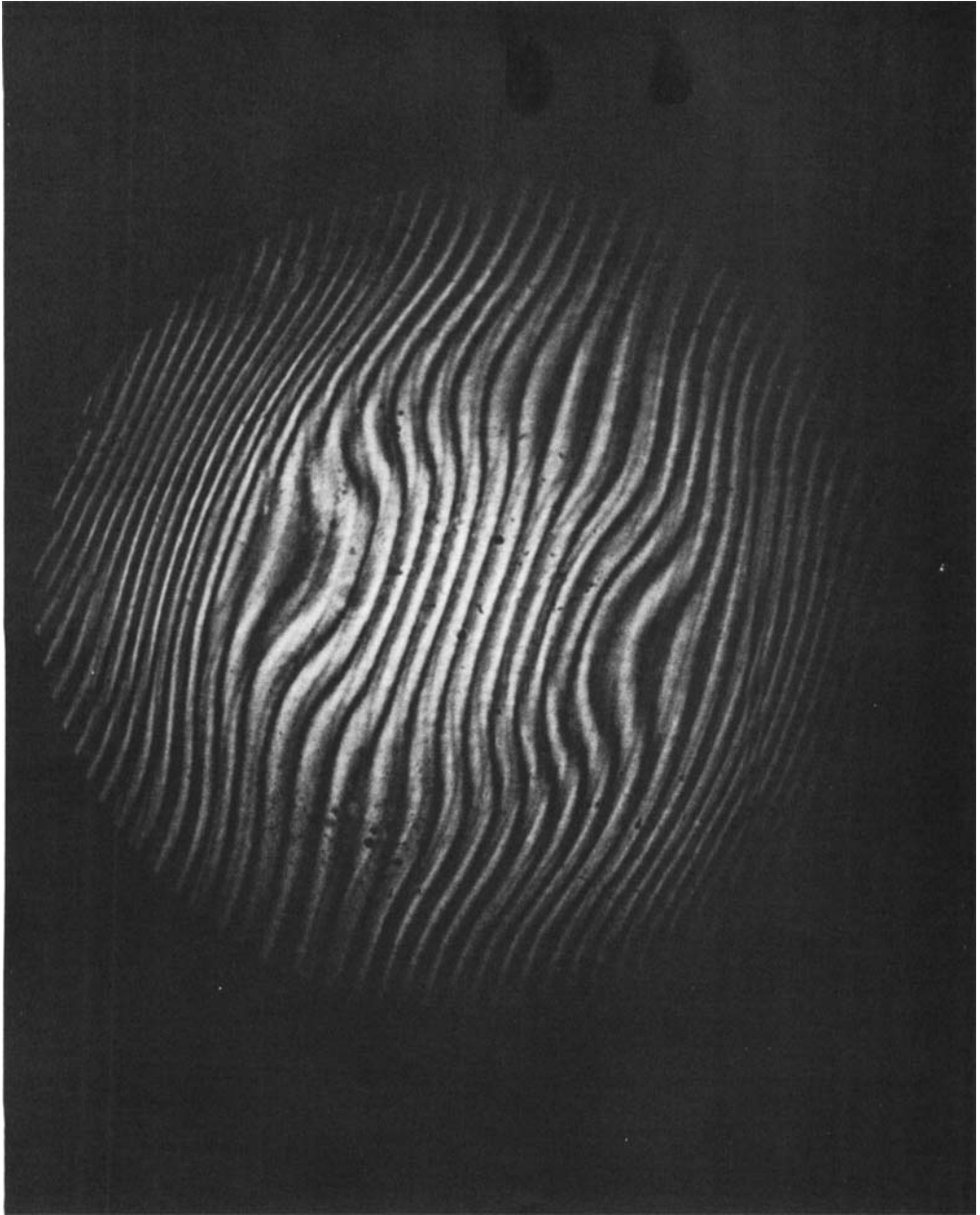


FIGURE 4. Thermal convection in the isotropic phase alone.  $\Delta T = 2^\circ\text{C}$ . Wider spacing between the interference lines indicates cooler temperatures.

shown in figure 3 for the conditions when  $\Delta T = 2^\circ\text{C}$  and the hotter temperature is just below the phase-change temperature,  $T_c$ . Upflow at the centre and second ring with downflow at the first ring and the outer edge is confirmed by direct observation with a stereo microscope. Small dust particles can easily be followed as they are carried by the fluid. With the same  $\Delta T$  and the colder temperature just above  $T_c$ , i.e. in the

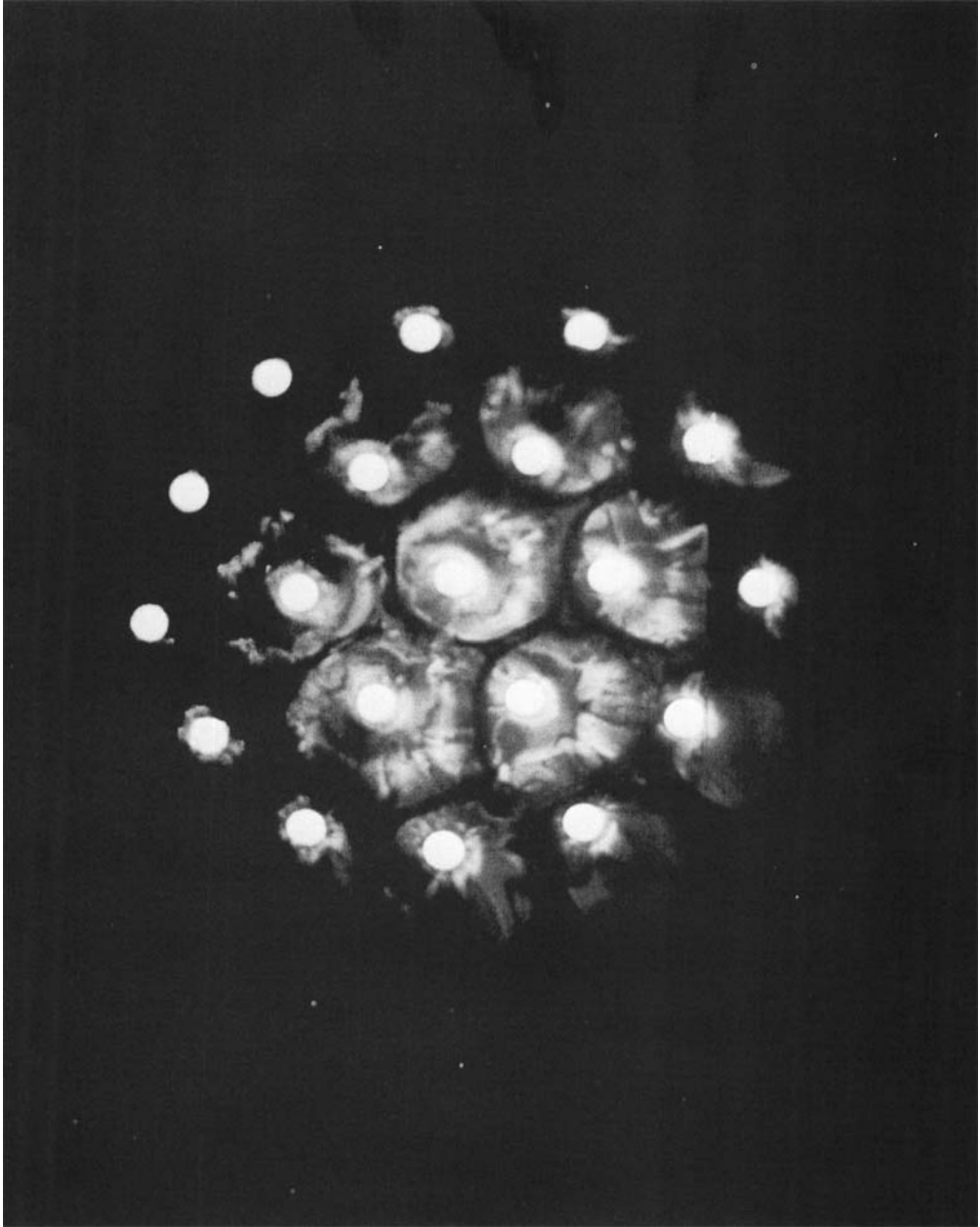


FIGURE 5. Buoyant motions due to unstable interface. Upshooting plumes from the thin layer of light fluid near the lower boundary create cellular motion.  $\Delta T = 0.1$  °C.

isotropic phase, the thermal pattern is seen to be just the same as for the heavier phase. A photograph of the interference pattern is shown in figure 4, where the wider spacing between bright lines indicates colder temperature. Careful observation of the interference pattern (and the associated shadowgraph) indicates that the diameter of the coldest part of the convection roll is just the same as for the other phase. A roll-like



pattern is always observed in thermal convection in just one phase. When the rotational symmetry of the flow is disturbed by inverting the cell and shaking it, the roll pattern that occurs once the layer is returned to horizontal is no longer circular, and sinuous rolls with spacing  $\lambda \sim 2d$  are observed.

The circular thermal pattern of the convection rolls is first seen in the lighter phase when  $\Delta T \lesssim 1.5^\circ\text{C}$ . When  $\Delta T = 2^\circ\text{C}$  the rolls are vigorous and the thermal pattern is quite distinct. In the heavier liquid-crystal phase the roll pattern is seen to start as  $\Delta T$  is raised above  $0.5^\circ\text{C}$  and to persist once started until  $\Delta T$  is lowered to  $0.3^\circ\text{C}$ . It appears, therefore, that the anisotropies of the liquid-crystal phase have lowered the critical temperature slightly, but the two visualization techniques do not necessarily have the same threshold, so a definite conclusion cannot be made. The hysteresis that occurs in the liquid-crystal phase is very slight, being almost within the precision of the temperature measurement.

Certainly, the effects of nematic anisotropy do not dominate the flow and do not result in a flow that is qualitatively different from that observed in the isotropic phase. With  $\Delta T = 2^\circ\text{C}$  the convection flow is the same in either phase, as nearly as can be determined. It is thus inferred that the liquid-crystal anisotropies have only a slight effect on the fluid motions to be described below.

### 3. Rayleigh–Taylor instability in the two-phase system

A statically unstable condition can be produced in a nearly isothermal layer, either by slightly elevating the lower temperature when the whole fluid layer is in the heavier phase at  $T_c$ , or by slightly lowering the upper temperature when the whole fluid is in the lighter phase at  $T_c$ . In the first case a thin layer of lighter fluid forms at the bottom, and in the second a thin layer of heavier fluid forms at the top. As the depth of the thin layer gets larger, the interface is seen to become distorted, finally leading to spouts of fluid shooting out of the thin layer. The spout of unstable fluid thus formed becomes the centre of a cellular pattern that continues to have a convective flow. The flow is quasi-steady with new cells starting up and old ones dying out but always with approximately the same spacing.

Figure 5 is a photograph of the monochromatic light transmitted through the cellular pattern that is formed when the cell is initially all nematic at  $T_c$  and is changed so that the lower temperature is  $0.1^\circ\text{C}$  above  $T_c$ . The bright circles are regions of upshooting out of the layer of clear, light fluid near the lower boundary. The slow return flow is along the boundaries of the cell. A parcel of fluid thus starts in the light phase, shoots up in the centre, spreads out along the slightly cooler top boundary changing to the heavy phase, and then returns to the centre of the cell to commence another trip. Figure 6 is the corresponding photograph of the pattern when the cell is initially all isotropic at  $T_c$  and is changed so that the upper boundary is  $0.1^\circ\text{C}$  lower than  $T_c$ . The darker circles are downshooting heavier fluid at the centre of the cells.

A sketch of the flow patterns is presented in figure 7, based on observations with the stereo microscope. It is seen that sinking motion is associated with changing from heavy to light (taking in latent heat), and rising motion with changing from light to heavy (giving off latent heat). This behaviour is as expected in the qualitative discussion in the introduction and is confirmed by watching the phase-change process. When  $\Delta T = 0$  and a parcel of fluid is changing from heavy to light (melting) it always sinks,

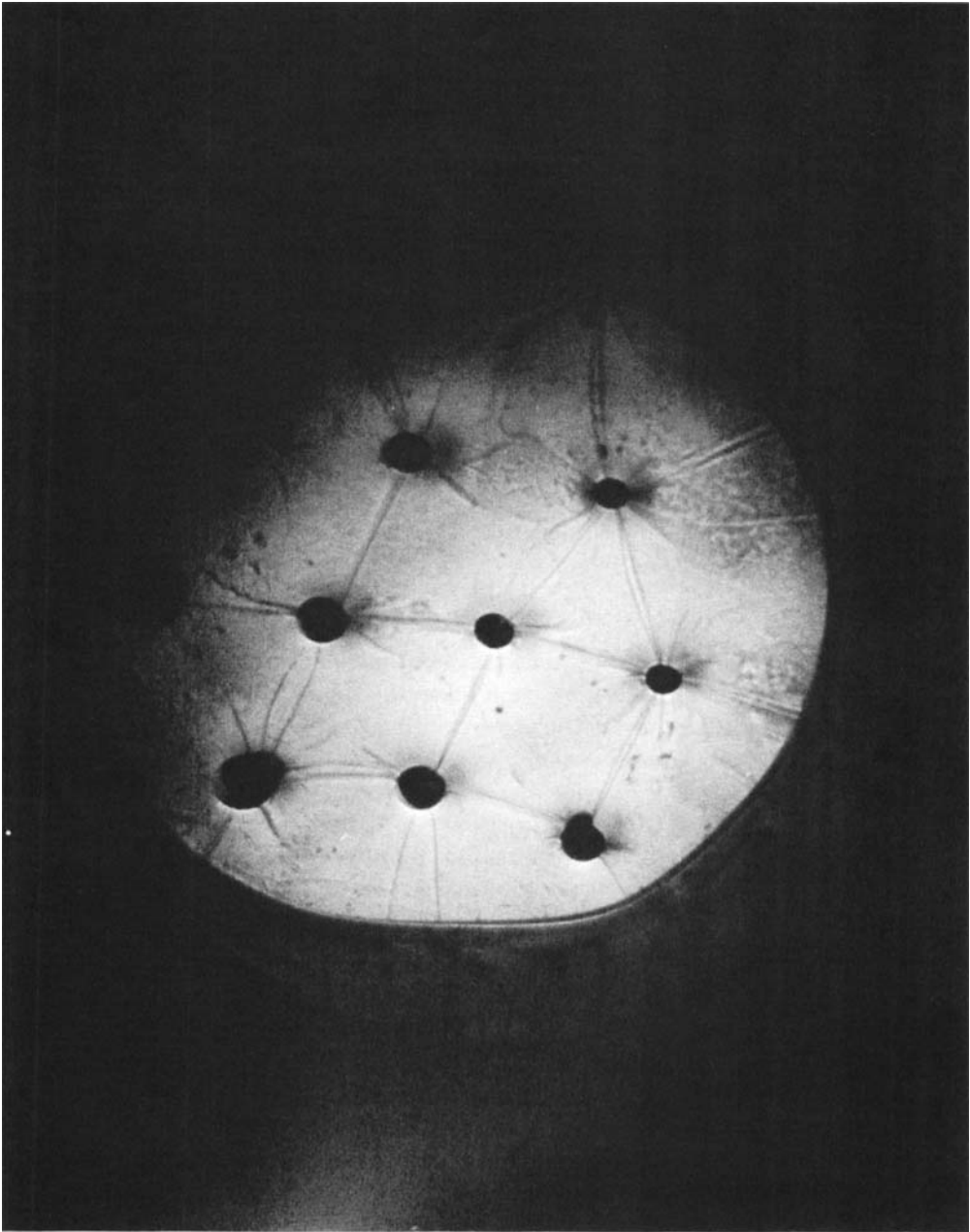


FIGURE 6. Buoyant motions due to unstable interface. Downshooting plumes from the thin layer of heavy fluid near the upper boundary create cells with downgoing centres.  $\Delta T = 0.1$  °C.

and when it is changing from light to heavy (freezing) it always rises. Thus, spheres of heavy fluid that are becoming larger rise, and those that are becoming smaller sink, when  $\Delta T = 0$ .

The initiation of the cellular motions is described by the analysis of Whitehead & Luter (1975), who have analyzed the linear Rayleigh–Taylor problem and speculated

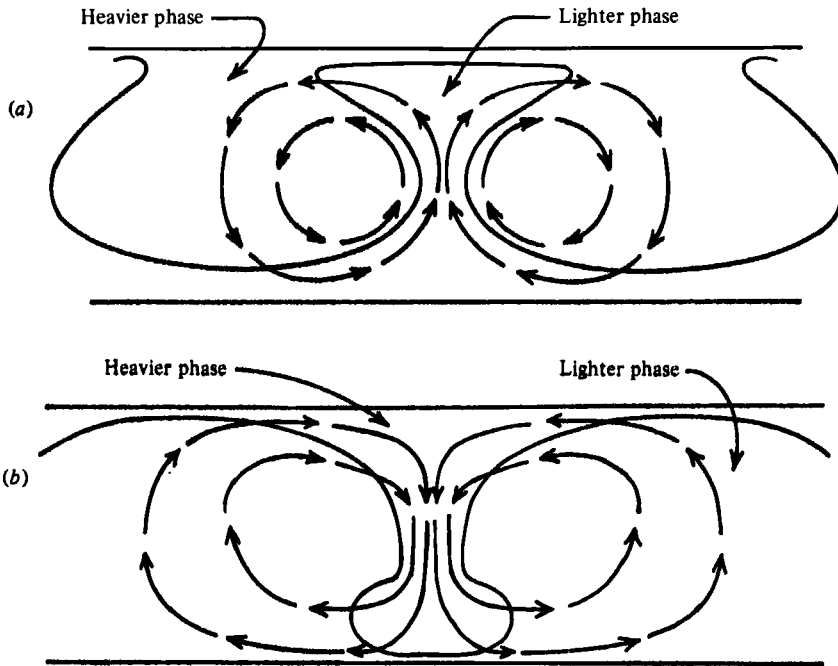


FIGURE 7. Sketch of cross-section of fluid cells shown in figures 5 and 6.

as to the finite-amplitude effects. The linear results for a thin layer of unstable fluid when the viscosities are equal indicate that the wavenumber of maximum growth is  $k = 2\pi/\lambda = 1.8/2h$ , and the growth rate is  $n = 0.15g(\Delta\rho/\rho)h/\nu$ , where  $h$  is the depth of thin layer. In the present case the calculated time for growth is 5 min when  $h = 0.1$  mm and 30 s when  $h = 1$  mm. Thus, when the layer depth has grown to 1 mm the instability should grow quickly, with a horizontal wavelength approximately equal to the depth of 6 mm. These are roughly the same values observed for both the upshooting and downshooting cells. Whitehead & Luther indicate that the planform of the motion should be hexagonal because of finite-amplitude effects, with the sign of the motion so that the fluid jets out of the thin layer. This result is also confirmed by the present results.

Once the motion has been established by the unstable density interface (corresponding to the parameter  $R_{\Delta\rho}$  discussed in the introduction), it continues without stopping. This is in contrast to the classic Rayleigh–Taylor problem where the fluid spout necks down where it started and becomes a bubble at the other boundary. The continuing flow must be due to the effect of latent heat release, which is of the proper sense and magnitude. But the fact that this latent-heat driven convection needs the finite-amplitude Rayleigh–Taylor flow to kick it off and a small temperature gradient to keep it going would surely complicate analysis of the flow.

#### 4. Combination of Rayleigh–Taylor and Rayleigh–Bénard instabilities

When an already-existing thermal convection flow in a single phase is altered by slightly changing the mean temperature (keeping  $\Delta T$  the same) so that the phase change occurs at one of the boundaries, the planform of the convection is immediately

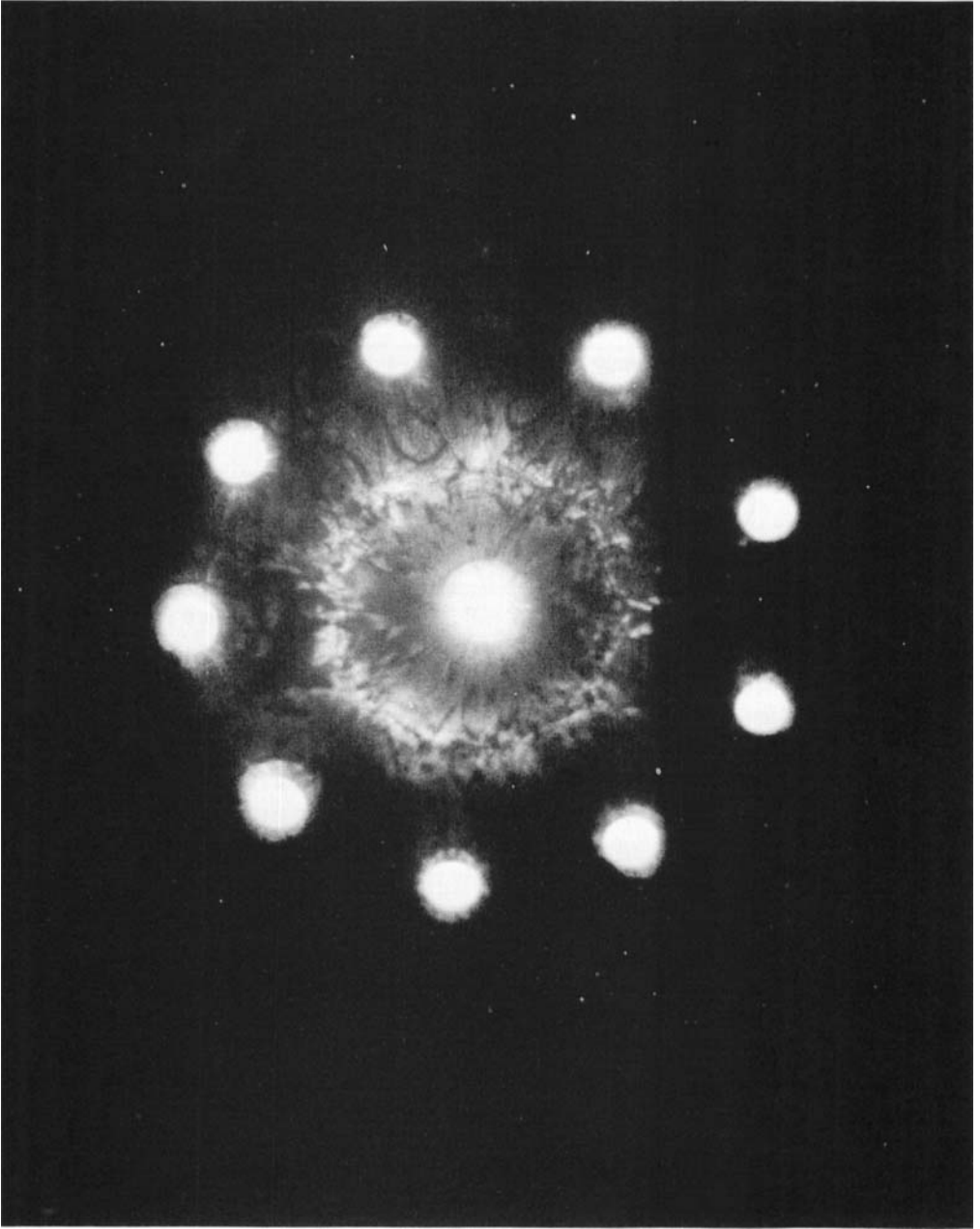


FIGURE 8. Thermal convection with phase change. Lower boundary is just above the phase-change temperature. Cells have upgoing centres.  $\Delta T = 2^\circ\text{C}$ .

altered. With the lower plate temperature just above  $T_c$ , the flow changes from rolls to cells with upshooting centres. This condition is shown in figure 8 where  $\Delta T = 2^\circ\text{C}$ . Parcels of fluid go right through the phase boundary as discussed in § 3, except with much greater speed. Because of the circular symmetry of the initial thermal convection flow the upshooting parts of the cells are arranged around the circle of upflow and the

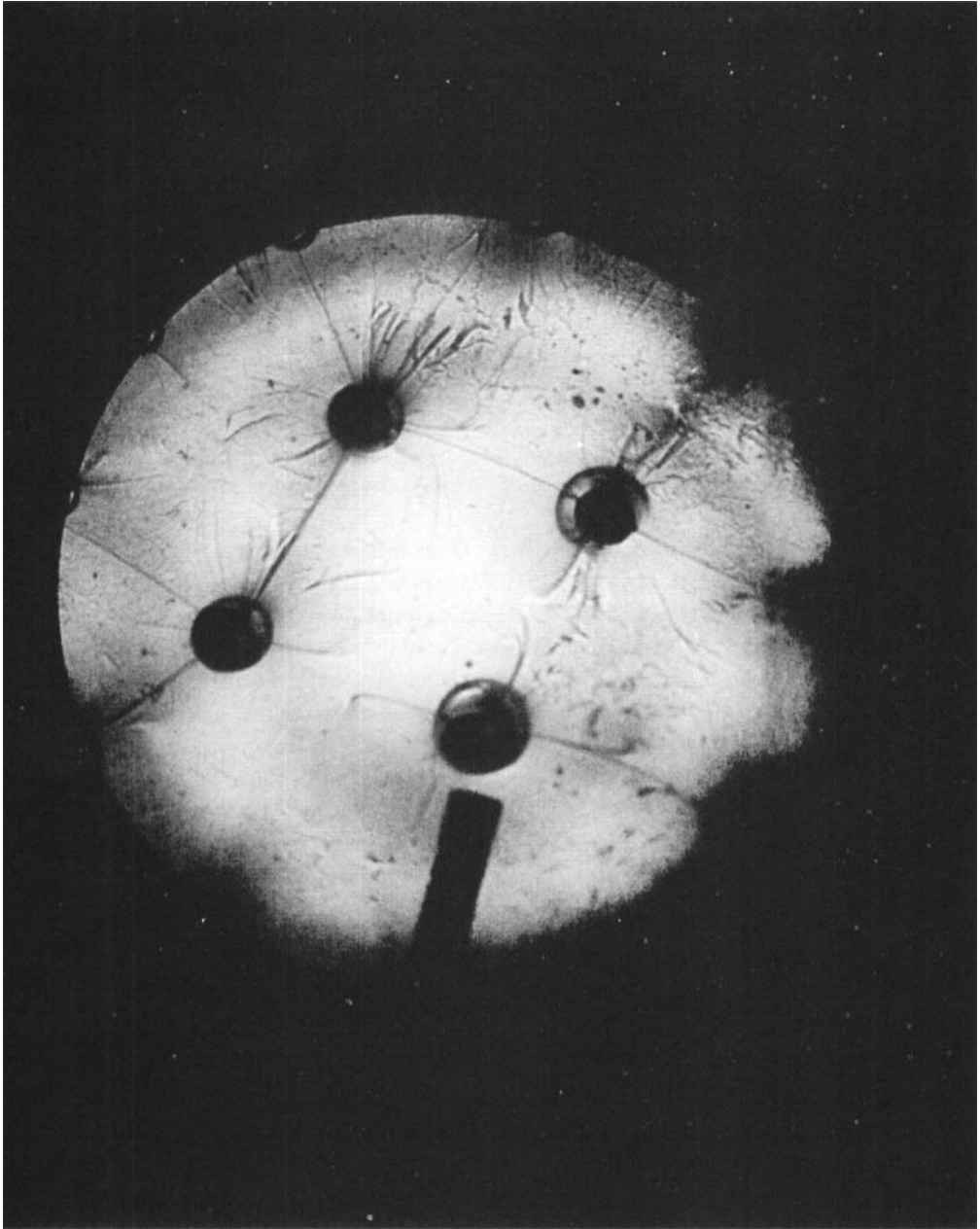


FIGURE 9. Thermal convection with phase change. Upper boundary is just below the phase-change temperature. Cells have downgoing centres.  $\Delta T = 2^\circ\text{C}$ . Length of dark bar is approximately twice the fluid depth.

centre. When the upper plate temperature is just below  $T_c$ , the cells have downshooting centres and are arranged around the downflow ring of the initial flow. This is shown in figure 9, where the dark line is approximately  $2d$ . In both cases, the flows are steady state, and the cellular motion is similar to the corresponding Rayleigh–Taylor flow (figures 5 and 6).

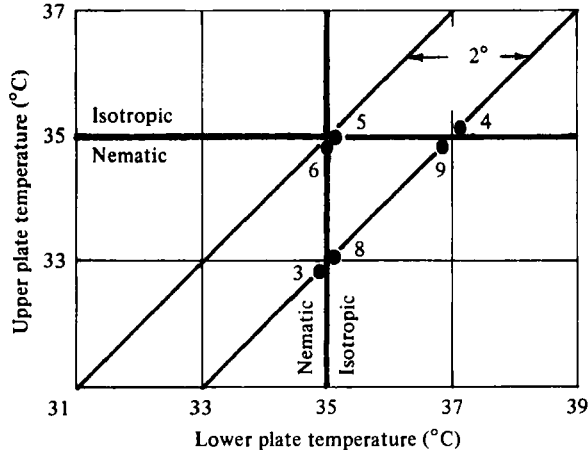


FIGURE 10. Regime diagram showing imposed temperatures for all the experiments. Numbers refer to the figure of the corresponding photograph.

The changing of the convection planform from rolls to hexagons when something is present to disturb the vertical symmetry of the flow is akin to the work of Busse (1962) for vertical variations in properties and Krishnamurti (1968, 1975) for time variations and boundary suction. In each case the vertically symmetric rolls must give way to the asymmetric hexagons. When convection occurs in a liquid, for example, the hexagons must have upshooting centres so that the jet occurs in the low-viscosity, warm fluid. Gas hexagons go the other way, because the low viscosity is in the cold fluid. In the two-phase convection the direction of motion in the cells indicates that the Rayleigh–Taylor instability provides asymmetry to cause the change in planform. The latent heat release is available to make the motion go faster, but since it is present in both updraft and downdraft, there is no contribution to asymmetry.

## 5. Summary and conclusions

The experimental conditions are summarized in figure 10. Thermal convection in each phase separately gave a basis with which to compare the two-phase results and showed that the anisotropies of the liquid-crystal working fluid did not greatly affect the results. When no appreciable thermal gradient was present and the phase boundary was unstable, the experimental results agree with the results of Whitehead & Luther (1975). The continuation of flow after its initiation by the unstable phase boundary is a new result and is unique to these experiments. The release of latent heat as the fluid passes through the phase boundary must be the primary cause of this quasi-steady flow. When thermal convection exists in the presence of a phase change, the planform was observed to be cellular, instead of the rolls in thermal convection alone. The cause of this change in planform is the vertical asymmetry due to fluid shooting out from the thin layer across the unstable interface.

The results have shown that a steady convection flow can exist right through a phase boundary, and that the flow is profoundly changed by the presence of a change of phase. However, the limits of the laboratory and complexity of the problem limit the applicability of these results to phase-change flows in geophysics, meteorology, and

astrophysics. The geophysical case that may be applicable to mantle convection, where the heavy fluid lies below, cannot be attained in the laboratory. Geological flows such as salt domes and volcanism are perhaps better modelled by fluids with vastly different viscosities, as used by Whitehead & Luther. The meteorological case of cumulus convection driven by latent heat release is certainly an important one and has been the object of previous laboratory experiments. In such a case, the release of latent heat occurs only in the updraft regions, which is different from the fluid used here.

In marine stratocumulus layers that are driven by latent heat release the density interface, i.e. the boundary between the marine layer and the free atmosphere, is a stabilizing influence (in contrast to the mantle convection where latent heat is stabilizing and the density interface destabilizing). So the present results do not apply, because in each of these cases the principal driving forces are in the wrong sense relative to each other. It appears that the fluid used in these experiments cannot be used to directly model geophysically relevant experiments. However, the results do show that the latent heat released in the phase change can keep the fluid in motion when it would ordinarily die out; and the density difference across the phase boundary can change the usual convection rolls to cells. Both these effects are similar to those that likely occur when phase change is present in geophysical or meteorological convection flows.

The author is grateful for the interest, encouragement and help of the staff of the following institutions: Woods Hole Oceanographic Institution, Geophysical Fluid Dynamics Summer Programme, University of California, Los Angeles Institute of Geophysics and Planetary Physics, University Colorado Department Astrogeophysics, University of California Davis Department Land, Air, and Water Resources, and NASA Marshall Space Flight Center Atmospheric Science Division.

#### REFERENCES

- BUSSE, F. H. 1962 Das Stabilitätsverhalten der Zellularkanvektion bei endlicher Amplitude. Ph.D. thesis, Ludwig-Maximilian University, Munich. (English translation by S. H. Davis Ref. LT-66-19 Rand. Corp. Santa Monica 1966.)
- BUSSE, F. H. & SCHUBERT, G. 1971 Convection in a fluid with two phases. *J. Fluid Mech.* **46**, 801-812.
- DUBOIS-VIOLETTE, E. & MANNEVILLE, P. 1978 Stability of Couette flow in nematic liquid crystals. *J. Fluid Mech.* **89**, 273-303.
- FITZJARRALD, D. E. & OWEN, E. W. 1979 Liquid crystal convection: a novel accelerometer. *J. Phys. E, Sci. Instrum.* **12**, 1075-1082.
- DE GENNES, P. G. 1974 The physics of liquid crystals. Clarendon Press.
- GUYON, E. & PIERANSKI, P. 1974 Convective instabilities in nematic liquid crystals. *Physica* **73**, 184-194.
- GUYON, E., PIERANSKI, P. & SALAN, J. 1979 Overstability and inverted bifurcation in homeotropic nematics heated from below. *J. Fluid Mech.* **93**, 65-81.
- HORN, D., GUYON, E. E. & PIERANSKI, P. 1976 Convection thermique dans les cellules nématiques inclinées. *Revue Phys. Appl.* **11**, 139-142.
- KNOPOFF, L. 1964 The convection current hypothesis. *Rev. Geophys.* **2**, 89.
- KRISHNAMURTI, R. 1968 Finite amplitude convection with changing mean temperature. *J. Fluid Mech.* **33**, 445-463.
- KRISHNAMURTI, R. 1975 On cellular cloud patterns. *J. Atmos. Sci.* **32**, 1353-1383.

- SCHUBERT, G. & TURCOTTE, D. L. 1971 Phase changes and mantle convection. *J. Geophys. Res.* **76**, 1424-1432.
- SCHUBERT, W. H., WAKEFIELD, J. S., STEINER, E. J. & COX, S. K. 1979 Marine Stratocumulus convection. *J. Atmos. Sci.* **36**, 1286-1324.
- SPEIGEL, E. A. 1972 Convection in stars. *Am. Rev. Astronomy & Astrophys.* **10**, 261-304.
- WHITEHEAD, J. A. & LUTHER, D. S. 1975 Dynamics of laboratory diapir and plume models. *J. Geophys. Res.* **80**, 705-717.